

Article

Effect of Addition of Zero-Valent Iron (Fe) and Magnetite (Fe₃O₄) on Methane Yield and Microbial Consortium in Anaerobic Digestion of Food Wastewater

Jun-Hyeong Lee ¹, Jae-Hyuk Lee ¹, Sang-Yoon Kim ² and Young-Man Yoon ^{1,3,*} 

¹ Department of Plant Life & Environmental Science, Hankyong National University, Anseong 17579, Republic of Korea

² School of Animal Life Convergence Science, Hankyong National University, Anseong 17579, Republic of Korea

³ Biogas Research Center, Hankyong National University, Anseong 17579, Republic of Korea

* Correspondence: yyman@hknu.ac.kr; Tel.: +82-31-670-5086

Abstract: Direct interspecies electron transfer (DIET), which does not involve mediation by electron carriers, is realized by the addition of conductive materials to an anaerobic digester, which then activates syntrophism between acetogenic and methanogenic microorganisms. This study aimed to investigate the effect of the addition of two conductive materials, zero-valent iron (ZVI) and magnetite, on the methane production and microbial consortium via DIET in the anaerobic digestion of food wastewater. The operation of a batch reactor for food wastewater without the addition of the conductive materials yielded a biochemical methane potential (B_u), maximum methane production rate (R_m), and lag phase time (λ) of 0.380 Nm³ kg⁻¹-VS_{added}, 15.73 mL day⁻¹, and 0.541 days, respectively. Upon the addition of 1.5% ZVI, B_u and R_m increased significantly to 0.434 Nm³ kg⁻¹-VS_{added} and 19.63 mL day⁻¹, respectively, and λ was shortened to 0.065 days. Simultaneously, *Methanomicrobiales* increased from 26.60% to 46.90% and *Methanosarcinales* decreased from 14.20% to 1.50% as the ZVI input increased from 0% to 1.50%. Magnetite, at an input concentration of 1.00%, significantly increased the B_u and R_m to 0.431 Nm³ kg⁻¹-VS_{added} and 18.44 mL day⁻¹, respectively. However, although magnetite improves the efficiency of methanogenesis via DIET, the effect thereof on the methanogen community remains unclear.

Keywords: anaerobic digestion; direct inter species electron transfer; zero valent iron; magnetite; methanogen



Citation: Lee, J.-H.; Lee, J.-H.; Kim, S.-Y.; Yoon, Y.-M. Effect of Addition of Zero-Valent Iron (Fe) and Magnetite (Fe₃O₄) on Methane Yield and Microbial Consortium in Anaerobic Digestion of Food Wastewater. *Processes* **2023**, *11*, 759. <https://doi.org/10.3390/pr11030759>

Academic Editor: Andrea Petrella

Received: 10 February 2023

Revised: 26 February 2023

Accepted: 2 March 2023

Published: 4 March 2023



Copyright: © 2023 by the authors. Licensee MDPI, Basel, Switzerland. This article is an open access article distributed under the terms and conditions of the Creative Commons Attribution (CC BY) license (<https://creativecommons.org/licenses/by/4.0/>).

1. Introduction

As of 2020, the amount of food waste generated in Korea was reported to be 5,160,000 tons per year, with more than 95% of food waste being utilized as resources for feeding and composting processes [1]. These processes generate a large amount of food wastewater, which, because of its high organic content and high hydrolysis rates, is an excellent raw material for biogas production. Anaerobic digestion is an energy-efficient process as it consumes less energy and produces bioenergy as a final product. Notably, anaerobic digestion is also environmentally friendly because it is suitable for the decomposition of highly concentrated organic matter, such as food wastewater, and can minimize the generation of surplus sludge in the treatment process. Therefore, compared to other biological treatments or physical/chemical treatment technologies, anaerobic digestion is the preferred food wastewater treatment technology with regard to pollution prevention and renewable energy production [2].

Anaerobic digestion is a process in which organic matter is converted into biogas mainly composed of methane and carbon dioxide. The organic matter undergoes microbial chemical reactions (hydrolysis, acidogenesis, acetogenesis, and methanogenesis), in

which various anaerobic microorganisms participate, in a reduced state in the absence of oxygen. Importantly, the stable anaerobic digestion of food wastewater requires the activity and reaction rates of the anaerobic microorganisms involved in hydrolysis, acidogenesis, acetogenesis, and methanogenesis to be balanced. In turn, the balancing of the microbial reaction rates in anaerobic digestion depends on the mechanism of syntrophy (cross feeding) between microorganisms in each reaction phase. In particular, the problems that typically arise in the operation of anaerobic digesters are due to the imbalance of nutrient symbiosis among microorganisms. Indirect interspecies electron transfer (IIET) is a form of syntrophism in which hydrogen or formate, which are products of acetogenic microorganisms, act as electron carriers between methanogenic microorganisms. In general, methanogenic microorganisms are sensitive to changes in environmental conditions, such as the concentration of organic acids, pH, temperature, and organic loading rates. Therefore, changes in these operational conditions within which anaerobic digesters operate affect the activity of methanogens, and for acetogenic microorganisms, the IIET mechanism is often found to be the problem. In particular, in the anaerobic digestion of highly concentrated biodegradable organic materials, such as food wastewater, hydrolysis, acidogenesis, and acetogenesis reactions proceed rapidly and lead to the accumulation of volatile fatty acids (VFAs). This phenomenon is problematic because it reduces the operational safety of anaerobic digesters. Specifically, the accumulation of these VFAs lowers the pH in the anaerobic digester, and the biogas conversion efficiency drops sharply owing to the inhibition of the IIET mechanism because of the decreased activity of the methanogens [3–5]. Therefore, the efficiency of anaerobic digestion is improved by promoting direct interspecies electron transfer (DIET) reactions, which do not depend on mediation by electron carriers such as hydrogen or formate, by adding conductive materials to anaerobic digesters [6,7].

Conductive materials that promote DIET include iron-based conductive materials, such as zero-valent iron (ZVI), magnetite, hematite, and ferrihydrite, and carbon-based conductive materials (biochar, carbon cloth, graphite, etc.). In iron-based conductive materials, iron occurs in various oxidation states (Fe^0 , Fe^{2+} , Fe^{3+} , etc.) [8,9]. The iron present in cytochromes, such as c-type cytochromes and F_{420}H_2 oxidase, plays an important role in methanogenesis [10,11]. In an anaerobic environment where alkaline conditions prevail, Fe^0 is oxidized to Fe^{2+} , and H^+ is reduced in the presence of Fe^0 with the production of H_2 by hydrogenotrophic methanogens. Although hydrogen is produced, it is continually consumed by these methanogens; consequently, low hydrogen partial pressure is maintained [12]. In addition, Fe^0 promotes the resistance of the methanogens to ammonia or acetic acid by increasing the number of ammonia-resistant *Methanoculleus* (hydrogenotrophic methanogen) species [13]. In addition, by promoting the DIET reaction, Fe^0 can induce the accumulation of *Syntrophomonas* and *Methanosaeta* to improve methane production [14]. As such, electron transfer between acetogenic and methanogenic microorganisms can be activated by the addition of conductive materials, and the improvement of the DIET reaction's efficiency prevents the accumulation of VFAs and induces efficient methane production, with an expected improvement in anaerobic digestion efficiency [15–20]. However, studies on DIET involving the addition of conductive materials have reported different anaerobic digestion enhancement efficiencies depending on the type of substrates, the type of conductive materials, the initial concentration of the additive in the digester, the timing of the addition, etc. Additionally, the acceleration of hydrolysis, acidogenesis, and acetogenesis inhibits methane production [21–24]. In particular, previous studies on DIET focused on evaluating the effect of the improvement of the methane yield by adding conductors, including granular activated carbon, biochar, ZVI, magnetite, hematite, and graphene, on the processing of simple substrates, such as glucose, propionate, and ethanol. There are a few studies on the application of the DIET reaction to the anaerobic digestion of organic waste such as sewage sludge and pig slurry. When $5\text{--}9\text{ mg g}^{-1}\text{-VS}$ of ZVI nanoparticles was added to sewage sludge, the biochemical methane potential increased to a maximum yield of $0.238\text{ Nm}^3\text{ kg}^{-1}\text{-VS}_{\text{added}}$ [25], and it was reported of the semi-continuous anaerobic digestion of sewage sludge that a higher dose (4.33 g L^{-1}) sustained positive effects for

a longer time, along with higher methane content, and a marked increase in the relative abundance of members of the *Methanothrix* genus, which was recognized as an acetoclastic species showing high affinity for acetate [26]. Furthermore, the addition (at 42, 84, 168, and 254 mg-ZVI g⁻¹-VSS) of ZVI nanoparticles at the time of methane production during the anaerobic digestion of pig slurry led to an increase in the average methane production rate of 165% and 94% in the thermophilic and mesophilic temperature ranges, respectively [27]. ZVI supplementation during the anaerobic digestion of ammonia-rich swine manure increased the efficiency of anaerobic digestion via the rapid growth of ammonia-tolerant hydrogenotrophic *Methanoculleus* species [13]. However, there are relatively few studies on the effect of ZVI on methane production during the anaerobic digestion of high-concentration organic matter such as food waste. In particular, because different types of food waste are present in varying compositions depending on the local food culture, each study has variable results, and there are hardly any studies on the application of DIET to food wastewater in Korea, whose food is characterized by its high starch and cellulose content but low protein and fat content [28]. Since the content of easily biodegradable organic matter is high in food waste, acid fermentation proceeds rapidly in the early stages of anaerobic digestion, which often causes operational problems in the anaerobic digestion of food waste. Therefore, DIET research may provide a technical alternative for the stabilization of food waste anaerobic digesters in Korea.

Therefore, herein, food wastewater, a major raw material for anaerobic digestion in Korea, was used as the substrate to characterize the DIET reaction in anaerobic digestion. In this study, we operated batch reactors by adding the conductive materials ZVI and magnetite. In addition, analyses of the methane yield (B_u), organic matter decomposition rate (VS_r), and maximum methane production rate (R_m) enabled us to examine the effect of ZVI and magnetite, which are conductive materials involved in DIET, on the anaerobic digestion reaction rate of food wastewater. Next-generation sequencing (NGS) was used to analyze the characteristics of the microbial community in the anaerobic reactors according to the type and concentration of additives comprising conductive materials.

2. Materials and Methods

2.1. Materials

The food wastewater used in this study was collected from a food-waste-recycling facility in Icheon. The physicochemical properties and elemental analysis results of the food wastewater used in this study are shown in Table 1. TS and VS in food wastewater were 102,422 and 89,756 mg L⁻¹, respectively.

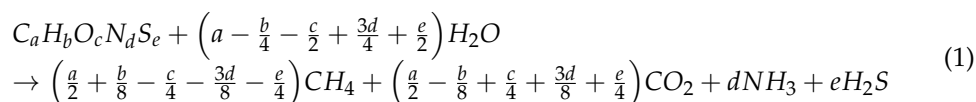
Table 1. Chemical composition and theoretical methane potential of food wastewater.

Parameter		Food Wastewater
pH (-)		3.53
TS ¹ (mg/L)		102,422
VS ² (mg/L)		89,756
TKN ³ (mg/L)		3870
NH ₄ ⁺ -N ⁴ (mg/L)		381
COD _{Cr} ⁵ (mg/L)		166,333
SCOD _{Cr} ⁶ (mg/L)		5474
TVFAs ⁷ (mg/L as acetate)		7657
Elemental composition (wt.%, d.b. ⁸)	C	46.70
	H	6.53
	O	3.27
	N	34.60
	S	0.00

All data correspond to the average values from three replicates (n = 3). ¹ Total solid, ² Volatile solid, ³ Total Kjeldahl nitrogen, ⁴ Ammonium nitrogen, ⁵ Chemical oxygen demand, ⁶ Soluble oxygen demand, ⁷ Total volatile fatty acids, ⁸ and Dry basis.

2.2. Methane Production Potential

The food wastewater used in this study was collected from a food-waste-recycling facility in Icheon. The theoretical methane potential was calculated stoichiometrically, using Boyle's (1976) equation for the decomposition reaction of organic matter (Equation (1)) based on the elemental analysis results of the published sample. Based on the complete equation for the decomposition reaction of organic matter, the formula for calculating theoretical methane potential (Equation (2)) was used.



$$B_{th} \left(Nm^3 kg^{-1} - VS_{added} \right) = 22.4 \times \left[\frac{(4a + b - 2c - 3d - 2e)/8}{12a + b + 16c + 14d + 32e} \right] \quad (2)$$

Biochemical methane potential (BMP) was evaluated by conducting a BMP assay [29]. The BMP of the control batch and that of the batches to which ZVI and magnetite were added were analyzed using an anaerobic batch reactor under medium temperature (38 °C) conditions. The anaerobic inoculum used in this study was collected from a biogas plant located in Icheon, and the physiochemical characteristics of the inoculum are presented in Table 2. The batch reactor used for the BMP test consisted of a 250 mL serum bottle, and food wastewater was added to the reactor while dispensing 125 mL of inoculum. The amount of food wastewater used as input was adjusted such that the ratio of volatile solids in the food wastewater to inoculum solution (S/I ratio) was 0.5. The conductive materials used as additives for DIET were ZVI powder (particle diameter of 44 µm or less) (Thermo Scientific, Waltham, MA, USA, CAS No. 7439-89-6) and magnetite (Fe₃O₄) powder (particle diameter of 5 µm or less) (Samchun Chemicals Co., Ltd., Seoul, South Korea, CAS No. 1317-61-9). The concentrations of conductive materials were 0.25, 0.50, 1.0, and 1.5% (2.5, 5.0, 10.0, and 15.0 mg/g-VS, respectively) for ZVI (and magnetite), and these values were based on the effective capacity of the batch reactor. A control group without ZVI and magnetite was created, and a blank test was performed to calibrate the biogas generated by the inoculum itself. Blank tests were repeated three times for all treatment groups. After filling the headspace with N₂ gas, the batch reactor was completely sealed with a blue butyl rubber septum stopper and an aluminum crimp seal to maintain an anaerobic state. The contents of the anaerobic reactor were stirred once a day at 38 °C, and anaerobic digestion was carried out for 33 days in the convection incubator and manually mixed each day during the fermentation period.

Table 2. Chemical composition of inoculum.

Parameters	pH (-)	TS ¹	VS ²	TKN ³ (mg L ⁻¹)	NH ₄ ⁺ -N ⁴	COD _{Cr} ⁵	SCOD _{Cr} ⁶	Alkalinity (mg L ⁻¹ as CaCO ₃)	TVFAs ⁷ (mg L ⁻¹ as Acetate)
Inoculum	8.36	20,767	9511	3467	2746	6017	4930	12,975	41

All data correspond to the average value from three replicates (n = 3). ¹ Total solid, ² Volatile solid, ³ Total Kjeldahl nitrogen, ⁴ Ammonium nitrogen, ⁵ Chemical oxygen demand, ⁶ Soluble chemical oxygen demand, and ⁷ Total volatile fatty acids.

The biogas that was generated was measured using a water column gas volume meter, and the generated biogas was converted to dry gas in the standard state (0 °C, 1 atm) by correcting the temperature and moisture level (as shown in Equation (3)) to obtain the cumulative methane production curve. In Equation (3), V_{dry gas} is the volume of dry gas under standard conditions (0 °C, 1 atm); T is the operating temperature of the reactor; V_{wet gas at T °C} is the volume of wet gas at the operating temperature of the reactor (T, 38 °C); P is the atmospheric pressure at the time the volume of the gas was measured; and P_T is

the saturated water vapor pressure (mmHg) at T °C. In this study, P is considered to be 760 mmHg, and P_T was calculated as the pressure of the saturated water vapor at 38 °C [30].

$$V_{dry\ gas} = V_{wet\ gas\ T^{\circ}C} \times \frac{273}{(273 + T)} \times \frac{(P - P_T)}{760} \quad (3)$$

The modified Gompertz model (Equation (4)) was employed to interpret the progress of cumulative methane production [31]. This enabled the cumulative methane production data to be optimized using these equations [32]. Particularly, the modified Gompertz model was applied for the estimation of the lag phase time and maximum methane production rate.

$$M_t = P \times \exp \left\{ -\exp \left[\frac{R_m \cdot e}{P} (\lambda - t) + 1 \right] \right\} \quad (4)$$

where M_t is the cumulative amount of methane production (mL), t is the anaerobic fermentation time (days), P is the final methane production (mL), e is the exp, R_m is the maximum methane production rate (mL/day), and λ represents the lag growth phase time (days).

2.3. Analysis of Microbial Consortium

2.3.1. DNA Extraction and Quantification

DNA was extracted using a DNA kit (GD141-050 Gram positive, Biofact, Korea) according to the manufacturer's instructions. The extracted DNA was quantified using Quant-IT PicoGreen (Invitrogen).

2.3.2. Library Construction and Sequencing

Sequencing libraries were prepared according to the Illumina 16S Metagenomic Sequencing Library protocols to amplify the V5 and V6 regions. The input gDNA of 2 ng was PCR-amplified with 5x reaction buffer, 1 mM of dNTP mix, 500 nM each of the universal F/R PCR primers, and Herculase II fusion DNA polymerase (Agilent Technologies, Santa Clara, CA, USA). The reaction conditions for the 1st PCR cycle were as follows: 3 min at 95 °C for heat activation; then, 25 cycles of 30 s at 95 °C, 30 s at 55 °C, and 30 s at 72 °C; and a 5 min final extension at 72 °C. The universal primer pair with Illumina adapter overhang sequences was used for the first amplifications as follows: V5-F: 5'-TCGTCGGCAGCGTCAGATGTGTATAAGAGACAGCCTACGGGNGGCWGCAG-3', and V6-R: 5'-GTCTCGTGGGCTCGGAGATGTGTATAAGAGACAGGACTACHVGGGTATCTAATCC-3'. The 1st PCR product was purified with AMPure beads (Agencourt Bioscience, Beverly, MA). Following its purification, 2 µL of the 1st PCR product was amplified by PCR for final library construction containing the index using NexteraXT Indexed Primer. The cycle conditions for the 2nd PCR product were the same as those of the 1st PCR product except that 10 cycles were used. This PCR product was purified with AMPure beads. The final purified product was then quantified using qPCR according to the qPCR quantification protocol guide (KAPA Library Quantification kits for Illumina Sequencing platforms) and qualified using TapeStation D1000 ScreenTape (Agilent Technologies, Waldbronn, Germany). Paired-end (2 × 300 bp) sequencing was performed via MacroGen using the MiSeq™ platform (Illumina, San Diego, CA, USA).

2.4. Chemical Analysis

Elemental analysis (C, H, O, N, and S) was performed using an elemental analyzer (EA1108, Thermo Finnigan LLC, San Jose, CA, USA). The gas composition of the biogas was analyzed using gas chromatography machine (Clarus 680, PerkinElmer, Waltham, MA, USA) equipped with a thermal conductivity detector. A HaysepQ packed column (3 mm × 3 m, 80–100 mesh size) was used, and high-purity argon (Ar) gas was used as moving bed to perform the analysis at an injector temperature of 150 °C, a column oven temperature of 90 °C, and a detector temperature of 150 °C during operation at a flow rate of 30 mL/min [33]. The total solids (TS), volatile solids (VS), chemical oxygen demand (COD_{Cr}), soluble chemical oxygen demand (SCOD_{Cr}), total Kjeldahl nitrogen

(TKN) content, total ammonium nitrogen ($\text{NH}_4^+\text{-N}$) content, alkalinity, and total volatile fatty acids (TVFAs) were measured according to a standard analytical method [34]. The concentration of the solubilized Fe was determined in the digestate and the filtrate (from which TSS was removed) of digestate using inductively coupled plasma optical emission spectrometry (ICP-OES) (Avio 550 Max, PerkinElmer, USA).

2.5. Statistical Analysis

The statistical analysis of the results of this experiment was based on the general linear model of the SAS[®] program package (SAS ver. 9.4, SAS institute Inc., Cary, NC, USA), and the significant mean difference between treatments was determined using Duncan's multiple-range test ($p < 0.05$) [35].

3. Results and Discussion

3.1. Methane Yield and Reaction Kinetics

The results of the experiments in which the methane yield was optimized via the addition of ZVI were calculated from the conducted BMP assay with the modified Gompertz model. These results are plotted in Figure 1, and the results of the analysis of the decomposition rate of organic matter for each treatment are presented in Table 3. The B_u , R_m , and lag phase of growth (λ) of the control groups were $0.380 \text{ Nm}^3 \text{ kg}^{-1}\text{-VS}_{\text{added}}$, $15.73 \text{ mL day}^{-1}$, and 0.541 days, respectively. For the group treated via the addition of ZVI at amounts of 0.25, 0.50, 1.00, and 1.50%, the calculated results are as follows: a B_u of 0.418, 0.423, 0.425, and $0.434 \text{ Nm}^3 \text{ kg}^{-1}\text{-VS}_{\text{added}}$; an R_m of 19.09, 19.53, 20.32, and $19.63 \text{ mL day}^{-1}$; and a λ of 0.352, 0.395, 0.364, and 0.065 days, respectively. The group treated with ZVI showed a statistically significant increase in methane yield as the ZVI concentration of the input increased. For the group to which 1.50% of ZVI was added, the B_u and R_m increased the most by 14.21% and 24.79%, respectively, and λ was 87.99% lower. Yuan et al. [36] reported that for the control group used in their study on the anaerobic digestion of food waste, the R_m and λ were 37.54 mL h^{-1} and 11.69 h, respectively, and when 10 g L^{-1} ZVI was added, the R_m increased to 51.88 and 50.30 mL h^{-1} , respectively. The R_m increased by 38.20% during hydrolysis and acidogenesis and 33.99% during methanogenesis, while λ was found to be 5.00 and 6.73 h, which was shortened by 57.23 and 42.43%, respectively. In addition, it was reported that the reactor to which ZVI had been added contained a lower concentration of propionate than the control group, and the pH of the reactor increased as VFAs were consumed. Propionate, when accumulated in anaerobic reactors, is known to cause an imbalance in pH between the phases of acidogenesis and methanogenesis, which negatively affects the methanogenesis of anaerobic microorganisms. The addition of ZVI activates propionate's enzymatic activities by reducing the Gibbs free energy of acetate-related enzymes by 8.0–10.2% and lowers the oxidation reduction potential to limit the production of propionate. By adding ZVI, the degradation rate of propionate increased by 12–34%, and an increase in propionic-utilizing bacteria and homoacetogenic bacteria has been previously reported [37].

Wang et al. [38] added 1.0 and 10.0 g L^{-1} of ZVI to a control group to improve the anaerobic digestion of waste-activated sludge. The level of methane production in the control group was reported to be $66.8 \text{ mL g}^{-1}\text{-VSS}$ and increased by approximately 33.6% to $89.2 \text{ mL g}^{-1}\text{-VSS}$ at 1.0 g L^{-1} , whereas at 10.0 g L^{-1} , the level of methane production decreased by approximately 42.1% to $28.1 \text{ mL g}^{-1}\text{-VSS}$. Their study, therefore, concluded that the addition of ZVI generally increases methane production, but that excessive ZVI can inactivate anaerobic microorganisms because of the strong reducing power of iron. Moreover, iron corrosion causes the pH to deviate from the optimal pH in the digester, resulting in the inhibition of methane production [39–41]. Kong et al. [42] reported the following results. With respect to the anaerobic digestion of food waste with a high organic loading rate, the alkalinity and VFA/alkalinity of the digestive fluid in the group without ZVI were $15,875 \text{ mg-CaCO}_3 \text{ L}^{-1}$ and 0.5 or more. However, upon treatment with ZVI, the alkalinity was in the range of $13,000\text{--}14,000 \text{ mg-CaCO}_3 \text{ L}^{-1}$, and the VFA/alkalinity

was maintained below 0.05, which improved the operational stability of the digester. Thus, the methanogens were activated even at low levels of ZVI during the anaerobic digestion of food waste, which effectively inhibited the acidification of the digester. This suggests that, in the case of a substrate such as food wastewater with a fast reaction rate during the hydrolysis, acidogenesis, and acetogenesis phases, operational problems are often attributable to the acidification of digesters. However, overcoming this operational problem is expected to greatly improve the operational safety of digesters by increasing the reaction rate in the methanogenic phase with the addition of ZVI.

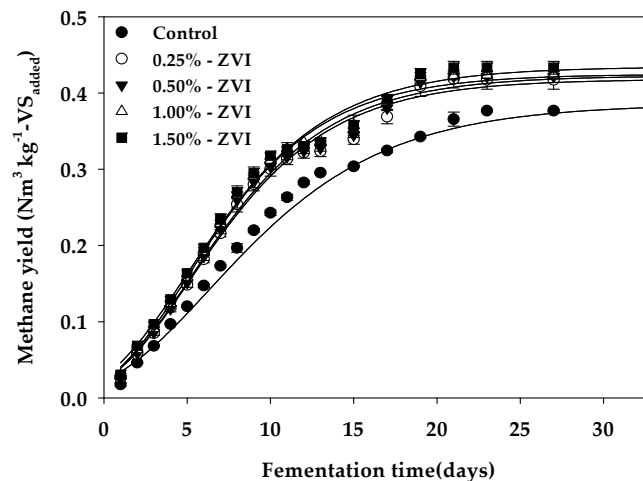


Figure 1. Methane yield curves optimized by the modified Gompertz model at different concentrations of zero-valent iron, Fe^0 (ZVI).

Table 3. Analysis of methane yield characteristics via the modified Gompertz model at different concentrations of zero-valent iron, Fe^0 (ZVI).

Parameters	Control	Zero-Valent Iron Concentration (%)			
		0.25	0.50	1.00	1.50
B_u ¹ ($\text{Nm}^3 \text{kg}^{-1} \text{VS}_{\text{added}}$)	0.380 c	0.418 b	0.423 ab	0.425 ab	0.434 a
R_m ² (mL day^{-1})	15.73 c	19.09 b	19.53 ab	20.32 a	19.63 ab
λ ³ (days)	0.541 a	0.352 b	0.395 b	0.364 b	0.065 c
B_{th} ⁴ ($\text{Nm}^3 \text{kg}^{-1} \text{VS}_{\text{added}}$)	0.437	0.437	0.437	0.437	0.437
VS_r ⁵ (%)	86.95	95.72	96.73	97.28	99.45

All data correspond to the average value from three replicates ($n = 3$). The mean values denoted by different letters differ significantly between treatments ($p < 0.05$). ¹ Biochemical methane potential, ² Maximum methane production rate, ³ Lag phase of growth, ⁴ Theoretical methane potential, and ⁵ Degree of degradation ($B_u/B_{th} \times 100$).

In our study, the cumulative methane production curves of the group treated with magnetite and optimized with the modified Gompertz model are shown in Figure 2, and the results of the analysis of the decomposition reaction rates of organic matter for each treatment group are presented in Table 4. At input concentrations of 0.25, 0.50, 1.00, and 1.50%, the group to which magnetite was added had B_u values of 0.411, 0.412, 0.431, and 0.419 $\text{Nm}^3 \text{kg}^{-1} \text{VS}_{\text{added}}$; R_m values of 15.94, 16.48, 18.44, and 18.26 mL day^{-1} ; and λ values of 0.469, 0.600, 0.673, and 0.650 days ($p < 0.05$). The methane yield of this group was the highest at an input concentration of 1.0%. At this concentration, the B_u and R_m increased by 10.26 and 16.08%, respectively, compared to the control group, while the λ was prolonged by 20.15%. Zhang et al. [43] reported that the R_m increased due to the activation of hydrogenotrophic methanogen by the addition of conductive materials; however, in the early stages of anaerobic digestion, the hydrogen partial pressure in the reactor remained high due to accelerated hydrogen production and the temporary inhibition of the activation

of hydrogenotrophic methanogen, thereby prolonging the λ . Their results support those of our study. The efficiency of the DIET reaction was determined by using various substrates to which magnetite was added as a conductor. Jing et al. [44] reported that the addition of 0, 0.01, 0.10, and 1.00 g L⁻¹ of magnetite to propionate as a substrate yielded 38.6 mL of methane and an R_m of 3.0 mL day⁻¹ for the control group. For the group treated with magnetite, methane production increased to 41.6, 40.7, and 42.7 mL, respectively, and the maximum methane production rate increased to 4.1, 4.3, and 4.1 mL day⁻¹, thus corroborating the results of our study. However, Jing et al. showed that the increase in B_u and R_m during the anaerobic digestion of propionate was the greatest when magnetite was added at a very low input concentration of 0.01 g L⁻¹, which differs from the results of our study. The food wastewater used as a substrate in our study has more complex substrate characteristics, including proteins, fats, etc., when compared with propionate. Therefore, in the case of propionate, even relatively low magnetite input concentrations markedly increased the B_u and R_m . In addition, Yin et al. [45] reported that when magnetite was added at 10 g L⁻¹ and a substrate comprising a mixture of soluble starch and tryptone was used, the lag phase growth was reduced by 20% compared to the control group and the R_m increased by 6.2%, and the COD removal rate increased by 23.8% in this process. Wang et al. [18] reported that when magnetite was added during the anaerobic digestion of sewage sludge at 0, 10, 50, and 100 mg g⁻¹-TS, the cumulative methane production of the group treated with magnetite increased after 20 days of reactor operation. However, the methane production did not increase when the magnetite input was increased. In contrast, another study reported that treatment with >50 mg g⁻¹-TS of magnetite increased the R_m . These previous studies led us to conclude that, in the case of composite substrates such as sewage sludge, the promotional effect of DIET as a result of the addition of various amounts of magnetite is unclear.

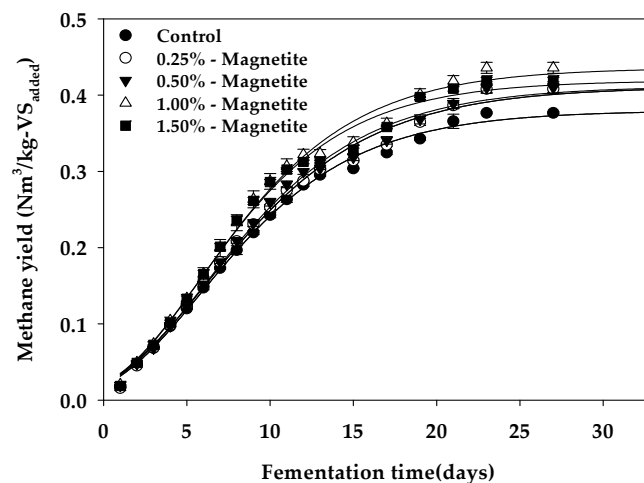


Figure 2. Methane yield curves optimized by the modified Gompertz model for the addition of different concentrations of magnetite (Fe_3O_4).

Nonetheless, many researchers have reported an increase in the efficiency of the DIET reaction via the addition of magnetite, while various inhibitory effects have also been observed. Akturk and Demier [46] reported that the addition of magnetite to food wastewater yielded a B_u of 293.0 mL g⁻¹-VS for the control group, yet the methane potential was reduced by 33.6 and 9.7% when magnetite with initial concentrations of 2.0 and 5.0 g/L was added. In addition, Straub et al. [47] reported that in anaerobic digestive fluid analysis, the sample group treated with ferrihydrite accumulated 10 mM of iron ions, whereas the groups to which magnetite and hematite were added accumulated less than 2 mM of iron ions. The high redox potential of ferrihydrite and the dissociative reduction of iron for the oxidation of electron donors (acetate, H_2) inhibit methane production. Thus, the results of various studies suggest that the efficiency of the DIET reaction with the addition of

conductive materials differs depending on the types of the substrates employed and the characteristics of the composition. Even the same iron-based conductive materials affected the efficiency of the DIET reaction differently, depending on the type and structure of the conductor.

Table 4. Analysis of methane yield characteristics by the modified Gompertz model at different concentrations of magnetite (Fe_3O_4).

Parameters	Control	Magnetite Concentration (%)			
		0.25	0.50	1.00	1.50
B_u ¹ ($\text{Nm}^3 \text{ kg}^{-1} \text{ VS}_{\text{added}}$)	0.380 c	0.411 b	0.412 b	0.431 a	0.419 b
R_m ² (mL day^{-1})	15.73 b	15.94 b	16.48 b	18.44 a	18.26 a
λ ³ (days)	0.541 ab	0.469 b	0.600 ab	0.673 a	0.650 a
B_{th} ⁴ ($\text{Nm}^3 \text{ kg}^{-1} \text{ VS}_{\text{added}}$)	0.437	0.437	0.437	0.437	0.437
VS_r ⁵ (%)	86.95	94.05	94.28	98.65	95.95

All data correspond to the average value from three replicates ($n = 3$). ^{a-c} Mean values denoted by different letters differ significantly between treatments ($p < 0.05$). ¹ Biochemical methane potential, ² Maximum methane production rate, ³ Lag phase of growth, ⁴ Theoretical methane potential, and ⁵ Degree of degradation ($B_u/B_{th} \times 100$).

3.2. Microbial Community

At the end of the BMP assay, the changes in the anaerobic microbial community were analyzed by using NGS on the anaerobic digestion sludge of the control group and the groups to which ZVI and magnetite had been added. The results of this analysis were summarized at the order and genus levels in the anaerobic microbial classification system (Figures 3 and 4). Analysis of the community distribution of methanogens with 0, 0.25, 0.50, 1.00, and 1.50% ZVI at the level of the order showed that the proportion of *Methanomicrobiales* increased to 26.60, 32.00, 39.50, 45.90, and 46.90%, whereas that of *Methanosarcinales* decreased to 14.20, 4.80, 2.70, 1.50, and 1.50% and that of *Methanobacteriales* decreased to 8.10, 5.60, 3.30, 2.20, and 2.20%. In addition, the quantity of *Methanomassiliicoccales* decreased to 1.60, 1.30, 0.80, 0.80, and 0.70%. In particular, the quantity of *Thermoanaerobacterales* involved in acetogenesis increased to 9.80, 13.70, 13.70, 10.70, and 10.00%, and *Eubacteriales* showed characteristics of a colonization level to 14.70, 11.30, 5.50, 5.10, and 5.30%. Analysis of the community characteristics of methanogens at the level of genus showed that the quantity of *Methanoculleus* increased to 26.50, 32.00, 39.50, 45.90, and 46.90% with an increase in ZVI concentration, while that of *Methanosarcinas* decreased to 12.80, 4.00, 2.20, 1.00, and 1.10%. The microbial distribution of *Methanosphaera*, *Methanobrevibacter*, and *Methanomassiliicoccus* decreased. The *Thermanaeromonas* involved in acetogenesis showed proportions of 9.50, 13.40, 13.60, 10.70, and 9.90% for ZVI concentrations of 0, 0.25, 0.50, 1.00, and 1.50%, respectively, and the microbial distribution of *Clostridium* and *Pelotomaculum* decreased with an increasing ZVI concentration. *Methanoculleus*, *Methanosphaera*, *Methanobrevibacter*, and *Methanomassiliicoccus* have been reported to be hydrogenotrophic methanogens that use H_2 and CO_2 as substrates, and *Methanosarcinas* have been reported to be mixotrophic methanogens producing CH_4 via CO_2 -reducing, methylotrophic, or acetotrophic pathways [48]. Based on these encouraging results, we added ZVI as a conductor for DIET, and resultantly, the microbial distribution of hydrogenotrophic methanogen increased significantly, whereas the microbial distribution of acetotrophic methanogen showed relatively less pronounced cluster characteristics. The distributions of acetate-producing bacteria (*Thermanaeromonas*, *Clostridium*, and *Pelotomaculum*) with methanogen and syntrophism were 18.10, 20.30, 16.70, 13.00, and 12.10% when ZVI was added in concentrations of 0, 0.25, 0.50, 1.00, and 1.50%, respectively. However, because of the continuous increase in the B_u and R_m with the increase in the initial amount of ZVI, the changes in the microbial distribution of acetate-producing bacteria (*Thermanaeromonas*, *Clostridium*, and *Pelotomaculum*) did not affect the DIET reaction. The group subjected to magnetite treatment showed neither an increasing nor a decreasing tendency for the generation of specific microorganisms in

response to the concentration of the magnetite additive compared to the control group and ZVI.

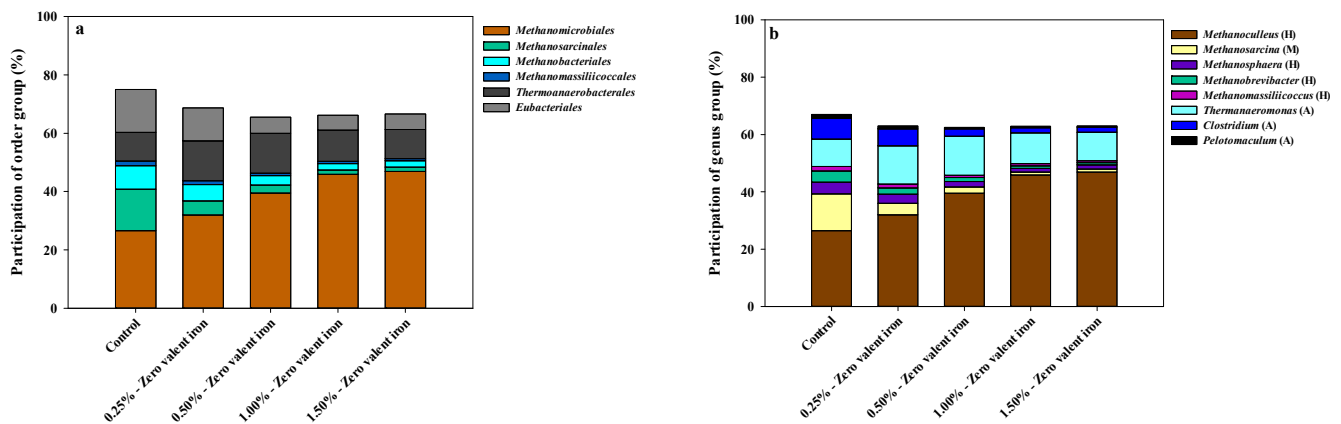


Figure 3. Taxonomic compositions of methanogens at the order level (a) and genus level (b) in the group treated with the additive zero-valent iron (Fe⁰), as retrieved from pyrosequencing (H, M, and A denote hydrogenotrophic methanogen, mixotrophic methanogen, and acidogenic bacteria, respectively).

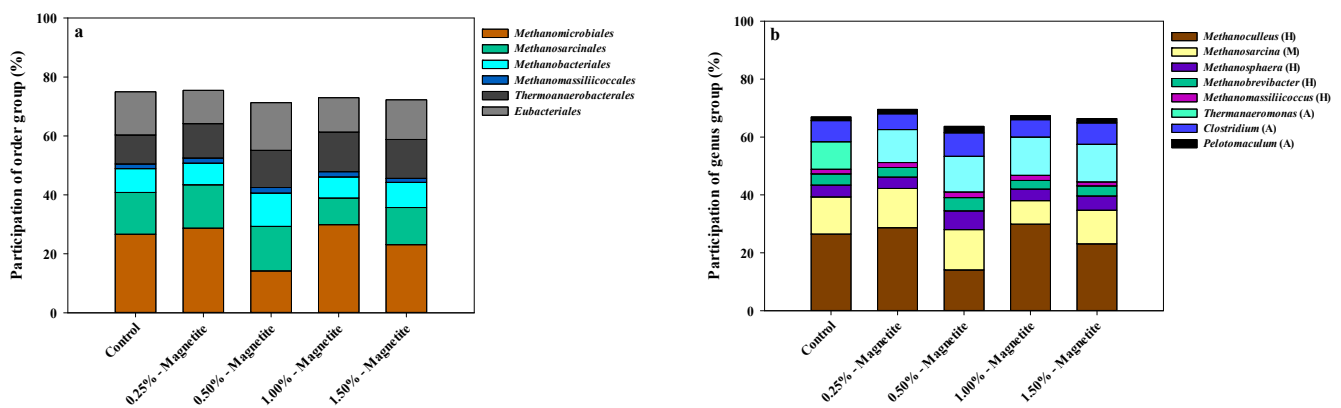


Figure 4. Taxonomic compositions of methanogens at the order level (a) and the genus level (b) in the group treated with magnetite (Fe₃O₄), as retrieved from pyrosequencing (H, M, and A denote hydrogenotrophic methanogen, mixotrophic methanogen, and acidogenic bacteria, respectively).

Table 5 shows the results of the analysis of the solubilized Fe content in the ZVI and magnetite treatment groups after the BMP assay was completed. Characteristically, the total solubilized Fe content and the soluble Fe content were high in the ZVI treatment group. Several methanogens can utilize ZVI as the sole electron donor [49], and methanogens can obtain electrons from ZVI faster than via hydrogen consumption [50]. In subsequent studies, ZVI was found to have beneficial effects on AD, including the stimulation of key enzymes in the acidification process and methanogenesis and a reduction in oxidation-reduction potential (ORP). Especially, ZVI can also produce H₂ by corrosion ($\text{Fe}^0 + 2\text{H}_2\text{O} \rightarrow \text{Fe}^{2+} + \text{H}_2 + 2\text{OH}^-$) [51]. H₂ is necessary for CO₂ conversion during methanogenesis. Therefore, ZVI was more easily oxidized than magnetite and showed a higher degree of solubilization. These oxidation characteristics of ZVI can provide a beneficial environment for hydrogenotrophic methanogen; for this reason, it is considered that the abundance of *Methanomicrobiales*, which are known as a hydrogenotrophic methanogen, increased with the ZVI treatment group to a greater extent than that of the magnetite treatment group.

Table 5. Concentration of the solubilized Fe in the ZVI and the magnetite (Fe₃O₄) treatment groups.

Treatments		Solubilized Fe	
		Soluble ¹ Forms	Total ² Forms
ZVI concentration (%)	0.25	27.0 (0.1) ³	530.4 (3.3)
	0.50	38.0 (0.3)	690.1 (1.4)
	1.00	30.1 (0.0)	606.3 (1.3)
	1.50	34.3 (0.0)	703.6 (1.1)
Magnetite concentration (%)	0.25	24.9 (0.1)	175.0 (0.1)
	0.50	23.5 (0.2)	182.0 (0.8)
	1.00	24.9 (0.1)	254.6 (0.8)
	1.50	25.3 (0.0)	214.9 (0.9)

¹ Fe determined in the filtrate of digestate, ² Fe determined in the digestate, and ³ Standard deviations (n = 3).

The increase in the microbial distribution of hydrogenotrophic methanogen with ZVI input has been reported by several researchers, and Yuan et al. [36] reported that when 10 g L⁻¹ ZVI was added to the anaerobic digester of food waste, the number of *Methanobacterium* (hydrogenotrophic methanogen) increased by 11.12% compared to the control group on day 31 of decomposition, and the energy recovery efficiency improved by promoting the rates of the methane production reactions. Studies on the DIET-promoting effects of various substrates other than food waste have also been reported. For example, Zheng et al. [52] added 5 g L⁻¹ of ZVI and magnetite to pig slurry. The methane potentials of the group to which ZVI and magnetite were added were 94.7 and 98.8 mL g⁻¹ -VS, amounting to an increase of 17.6 and 22.7%, respectively, compared to the control group (80.5 mL g⁻¹ -VS), and clearly demonstrating the increase in the methane potential enabled by conductive materials. At this time, the quantities of *Methanothrix* (acetotrophic methanogen) and *Methanolinea* (hydrogenotrophic methanogen) in the control group increased by 31.3 and 7.4%, respectively, whereas they increased by 37.5 and 8.6%, respectively, for the group treated with ZVI. In contrast, the colonization characteristics of the group to which magnetite had been added did not significantly depend on the concentration of the additive, which is similar to the results in the current study. In addition, Zhao et al. [53] showed that during the anaerobic digestion of sewage sludge, the colony distribution of the hydrogenotrophic methanogen in the control group was 31.8%, and when treated with 5 g L⁻¹ of ZVI, magnetite, and ZVI + magnetite, the colony distributions of the hydrogenotrophic methanogen were 43.8, 12.9, and 6.1%, respectively. Reportedly, treatment with magnetite resulted in a decrease in the distribution of hydrogenotrophic methanogen. When amounts of 0, 5, and 10 g L⁻¹ of biochar were added to food waste for anaerobic digestion, the colony distributions of *Methanosarcina thermophila* (mixotrophic methanogen) increased to 4.89, 6.15, and 10.30%, and those of *Methanoculleus receptaculi* (hydrogenotrophic methanogen) increased to 1.79, 5.66, and 6.22%, respectively, thereby increasing the overall methanogen colony distribution [54]. However, it was reported that a 5 g L⁻¹ biochar input increased the diversity of the microbial colonization, whereas an input concentration of 10 g L⁻¹ caused the populations of certain microbial colonies to decrease, thereby reducing the diversity of microbial colonization. According to these studies, the use of ZVI as a conductive material was accompanied by an increase in the colonization of hydrogenotrophic methanogen. However, the results of different studies suggest that the characteristics of microbial colonization varied with different conductive materials, input concentrations, and types of raw materials. Changes in microbial colonization characteristics are not necessarily affected by the promotion of DIET. Several research groups have reported colonization analyses of methanogens during the anaerobic digestion of food wastewater.

Jang et al. [55] reported that during the operation of batch anaerobic digesters for food wastewater, the portion of the *Methanosarcinales* colony (mixotrophic methanogen) decreased from 81.3% in the early stages of anaerobic digestion to 54% in the later stage, while *Methanomicrobiales* (hydrogenotrophic methanogen) increased from 11% in the initial stage of anaerobic digestion to 25% in the later stage. Lee et al. [56] reported that

Methanoculleus (hydrogenotrophic methanogen) accounted for 78.6% of the distribution in the operation of a continuous anaerobic digester of food wastewater, while that of *Methanosarcina* (mixotrophic methanogen) amounted to 1.2%. This indicates that the colony distribution of a methanogen during the anaerobic digestion of food waste also varies with the duration of the operation of the anaerobic digester. Therefore, the increase in the colony distribution of the hydrogenotrophic methanogen with respect to the addition of conductors for the anaerobic digestion of food may be a general trend in the operation of anaerobic digesters. The characteristics of the colonization change in the anaerobic food digester and the increase in the colony distribution of the hydrogenotrophic methanogen in response to the addition of a conductor are believed to be related.

4. Conclusions

With regard to the anaerobic digestion of organic matter, various syntrophic mechanisms are involved in the reaction stages of microorganisms. Of these mechanisms, DIET is a syntrophic mechanism that promotes electron transfer between acetogenic and methanogenic microorganisms by using conductive materials as mediators. In general, the anaerobic digestion of biodegradable organic matter such as food is problematic because the methane production phase is inhibited by the accumulation of organic acid, and the pH decreases due to the high rates of hydrolysis, acidogenesis, and acetogenesis. These problems adversely affect the operational stability of anaerobic digesters in commercialized biogas production facilities and, in turn, are major factors that cause these digesters to malfunction. An effective approach with which to alleviate these problems is to bolster the electron transfer reaction via DIET by adding conductors to increase the reaction rates of methanogens and promote the consumption of the substrate generated during acetogenesis, thereby maintaining the operational stability of the anaerobic digester. In particular, DIET is highly advantageous because it is a metabolic control method that can improve the methane production efficiency and operational stability of currently available anaerobic digesters without the incorporation of a separate process. This motivated our study, whose objective was to determine the effect of the addition of ZVI and magnetite on the anaerobic digestion efficiency and community characteristics of anaerobic microorganisms during the anaerobic digestion of food wastewater generated in Korea. In the ZVI treatment group, the B_u and R_m increased by 14.21 and 24.79%, respectively, and the B_u and R_m increased by 10.26 and 16.08%, respectively, in the magnetite treatment group, indicating that the addition of ZVI and magnetite significantly increased the methane production and reaction rates of anaerobic digestion. In addition, with respect to the characteristics of the microbial community, as the input concentration of ZVI increased, the distribution of hydrogenotrophic methanogen increased, and the distribution of acetotrophic methanogen decreased. Thus, the community characteristics of the methanogen changed with the promotion of the DIET reaction, although the change of these characteristics in response to the treatment with magnetite was unclear. Therefore, the use of ZVI and magnetite as additives in the anaerobic digestion of food wastewater was evaluated as a method of improving the operational stability of an anaerobic digester. However, ZVI had a DIET-promoting effect that affected the community characteristics of the methanogen, whereas with magnetite, the DIET-promoting effect did not affect these characteristics. Therefore, the extent to which ZVI, as a more efficient conductor than magnetite, changes the community characteristics of the methanogen was evaluated in terms of the operational stability of anaerobic digesters. However, the results of this study were obtained using a batch reactor. In particular, depending on the researchers, the degree of DIET promotion and the change in the characteristics of the microbial community were reported for different experimental conditions. Therefore, to apply the DIET promotion technology to commercialized biogas production facilities, it would be necessary to verify the reproducibility of the improvement in the methane production efficiency according to the addition of conductors. In addition, further research would be required to assess the expression of the DIET promotion effect and the conditions for expression in a continuous reactor.

Author Contributions: Conceptualization, Y.-M.Y.; methodology, J.-H.L. (Jun-Hyeong Lee) and Y.-M.Y.; software, J.-H.L. (Jae-Hyuk Lee) and S.-Y.K.; validation, J.-H.L. (Jun-Hyeong Lee) and Y.-M.Y.; formal analysis, J.-H.L. (Jae-Hyuk Lee) and S.-Y.K.; investigation, J.-H.L. (Jun-Hyeong Lee), J.-H.L. (Jae-Hyuk Lee), and S.-Y.K.; resources, Y.-M.Y.; data curation, Y.-M.Y.; writing—original draft preparation, J.-H.L. (Jun-Hyeong Lee); writing—review and editing, Y.-M.Y.; visualization, S.-Y.K.; supervision, Y.-M.Y.; project administration, Y.-M.Y.; funding acquisition, Y.-M.Y. All authors have read and agreed to the published version of the manuscript.

Funding: This study was supported by the MAFRA and IPET's support for industrialization technology development to respond to current livestock issues (Project NO. 321091-03).

Institutional Review Board Statement: Not applicable.

Informed Consent Statement: Not applicable.

Data Availability Statement: Not applicable.

Conflicts of Interest: The authors declare no conflict of interest. The funders had no role in the design of the study; in the collection, analyses, or interpretation of data; in the writing of the manuscript, or in the decision to publish the results.

References

1. ME [Ministry of Environment]. *National Waste Generation and Treatment Status [2020]*; Ministry of Environment: Sejong, Republic of Korea, 2021.
2. KEITI [Korea Environmental Industry & Technology Institute]. *Trends in Land Treatment of Food Wastewater*; Korea Environmental Industry & Technology Institute: Seoul, Republic of Korea, 2016.
3. Akindele, A.A.; Sartaj, M. The toxicity effects of ammonia on anaerobic digestion of organic fraction of municipal solid waste. *Waste Manag.* **2018**, *71*, 757–766. [\[CrossRef\]](#)
4. Li, L.; Xu, Y.; Dai, X.; Dai, L. Principles and advancements in improving anaerobic digestion of organic waste via direct interspecies electron transfer. *Renew. Sustain. Energy Rev.* **2021**, *148*, 111367. [\[CrossRef\]](#)
5. Müller, N.; Worm, P.; Schink, B.; Stams, A.J.; Plugge, C.M. Syntrophic butyrate and propionate oxidation processes: From genomes to reaction mechanisms. *Environ. Microbiol. Rep.* **2010**, *2*, 489–499. [\[CrossRef\]](#)
6. Morita, M.; Malvankar, N.S.; Franks, A.E.; Summers, Z.M.; Giloteaux, L.; Rotaru, A.E.; Rotaru, C.; Lovley, D.R. Potential for direct interspecies electron transfer in methanogenic wastewater digester aggregates. *MBio* **2011**, *2*, e00111–e00159. [\[CrossRef\]](#)
7. Rotaru, A.-E.; Shrestha, P.M.; Liu, F.; Markovait, B.; Chen, S.; Nevin, K.P.; Lovley, D.R. Direct interspecies electron transfer between *Geobacter metallireducens* and *Methanosarcina barkeri*. *Appl. Environ. Microbiol.* **2014**, *80*, 4599–4605. [\[CrossRef\]](#) [\[PubMed\]](#)
8. Lauderdale, J.M.; Braakman, R.; Forget, G.; Dutkiewicz, S.; Follows, M.J. Microbial feedbacks optimize ocean iron availability. *Proc. Natl. Acad. Sci. USA* **2020**, *117*, 4842–4849. [\[CrossRef\]](#)
9. Baek, G.; Kim, J.; Lee, C. A review of the effects of iron compounds on methanogenesis in anaerobic environments. *Renew. Sustain. Energy Rev.* **2019**, *113*, 109282. [\[CrossRef\]](#)
10. Seedorf, H.; Hagemeyer, C.H.; Shima, S.; Thauer, R.K.; Warkentin, E.; Ermler, U. Structure of coenzyme F₄₂₀H₂ oxidase (FprA), a di-iron flavoprotein from methanogenic Archaea catalyzing the reduction of O₂ to H₂O. *FEBS J.* **2007**, *274*, 1588–1599. [\[CrossRef\]](#) [\[PubMed\]](#)
11. Salgueiro, C.A.; Morgado, L.; Silva, M.A.; Ferreira, M.R.; Fernandes, T.M.; Portela, P.C. From iron to bacterial electroconductive filaments: Exploring cytochrome diversity using *Geobacter* bacteria. *Coord. Chem. Rev.* **2022**, *452*, 214284. [\[CrossRef\]](#)
12. Charalambous, P.; Vyrides, I. In situ biogas upgrading and enhancement of anaerobic digestion of cheese whey by addition of scrap or powder zero-valent iron (ZVI). *J. Environ. Manag.* **2021**, *280*, 111651. [\[CrossRef\]](#) [\[PubMed\]](#)
13. Yang, Y.; Yang, F.; Huang, W.; Huang, W.; Li, F.; Lei, Z.; Zhang, Z. Enhanced anaerobic digestion of ammonia-rich swine manure by zero-valent iron: With special focus on the enhancement effect on hydrogenotrophic methanogenesis activity. *Bioresour. Technol.* **2018**, *270*, 172–179. [\[CrossRef\]](#) [\[PubMed\]](#)
14. Jin, H.-Y.; He, Z.-W.; Ren, Y.-X.; Tang, C.-C.; Zhou, A.-J.; Liu, W.; Liang, B.; Li, Z.-H.; Wang, A. Current advances and challenges for direct interspecies electron transfer in anaerobic digestion of waste activated sludge. *Chem. Eng. J.* **2022**, *450*, 137973. [\[CrossRef\]](#)
15. Baek, G.; Kim, J.; Kim, J.; Lee, C. Role and potential of direct interspecies electron transfer in anaerobic digestion. *Energies* **2018**, *11*, 107. [\[CrossRef\]](#)
16. Kato, S.; Hashimoto, K.; Watanabe, K. Methanogenesis facilitated by electric syntrophy via (semi) conductive iron-oxide minerals. *Environ. Microbiol.* **2012**, *14*, 1646–1654. [\[CrossRef\]](#) [\[PubMed\]](#)
17. Tan, J.; Wang, J.; Xue, J.; Liu, S.-Y.; Peng, S.-C.; Ma, D.; Chen, T.-H.; Yue, Z. Methane production and microbial community analysis in the goethite facilitated anaerobic reactors using algal biomass. *Fuel* **2015**, *145*, 196–201. [\[CrossRef\]](#)

18. Wang, T.; Zhang, D.; Dai, L.; Dong, B.; Dai, X. Magnetite triggering enhanced direct interspecies electron transfer: A scavenger for the blockage of electron transfer in anaerobic digestion of high-solids sewage sludge. *Environ. Sci. Technol.* **2018**, *52*, 7160–7169. [\[CrossRef\]](#)
19. Zhao, Z.; Zhang, Y.; Woodard, T.; Nevin, K.; Lovley, D. Enhancing syntrophic metabolism in up-flow anaerobic sludge blanket reactors with conductive carbon materials. *Bioresour. Technol.* **2015**, *191*, 140–145. [\[CrossRef\]](#)
20. Zhuang, L.; Tang, J.; Wang, Y.; Hu, M.; Zhou, S. Conductive iron oxide minerals accelerate syntrophic cooperation in methanogenic benzoate degradation. *J. Hazard. Mater.* **2015**, *293*, 37–45. [\[CrossRef\]](#)
21. Aguilar-Moreno, G.S.; Navarro-Cerón, E.; Velázquez-Hernández, A.; Hernández-Eugenio, G.; Aguilar-Méndez, M.Á.; Espinosa-Solares, T. Enhancing methane yield of chicken litter in anaerobic digestion using magnetite nanoparticles. *Renew. Energy* **2020**, *147*, 204–213. [\[CrossRef\]](#)
22. Altamirano-Corona, M.F.; Anaya-Reza, O.; Durán-Moreno, A. Biostimulation of food waste anaerobic digestion supplemented with granular activated carbon, biochar and magnetite: A comparative analysis. *Biomass Bioenergy* **2021**, *149*, 106105. [\[CrossRef\]](#)
23. Li, D.; Song, L.; Fang, H.; Li, P.; Teng, Y.; Li, Y.-Y.; Liu, R.; Niu, Q. Accelerated bio-methane production rate in thermophilic digestion of cardboard with appropriate biochar: Dose-response kinetic assays, hybrid synergistic mechanism, and microbial networks analysis. *Bioresour. Technol.* **2019**, *290*, 121782. [\[CrossRef\]](#) [\[PubMed\]](#)
24. Yan, W.; Zhang, L.; Wijaya, S.M.; Zhou, Y. Unveiling the role of activated carbon on hydrolysis process in anaerobic digestion. *Bioresour. Technol.* **2020**, *296*, 122366. [\[CrossRef\]](#) [\[PubMed\]](#)
25. Lizama, A.C.; Figueiras, C.C.; Pedreguera, A.Z.; Espinoza, J.E.R. Enhancing the performance and stability of the anaerobic digestion of sewage sludge by zero valent iron nanoparticles dosage. *Bioresour. Technol.* **2019**, *275*, 352–359. [\[CrossRef\]](#) [\[PubMed\]](#)
26. Barrera, R.; del Carmen Vargas-García, M.; Capell, G.; Barańska, M.; Puentes, V.; Moral-Vico, J.; Sánchez, A.; Font, X. Sustained effect of zero-valent iron nanoparticles under semi-continuous anaerobic digestion of sewage sludge: Evolution of nanoparticles and microbial community dynamics. *Sci. Total Environ.* **2021**, *777*, 145969. [\[CrossRef\]](#) [\[PubMed\]](#)
27. Cerrillo, M.; Burgos, L.; Ruiz, B.; Barrera, R.; Moral-Vico, J.; Font, X.; Sanchez, A.; Bonmati, A. In-situ methane enrichment in continuous anaerobic digestion of pig slurry by zero-valent iron nanoparticles addition under mesophilic and thermophilic conditions. *Renew. Energy* **2021**, *180*, 372–382. [\[CrossRef\]](#)
28. ME [Ministry of Environment]. *Technical Guidelines for Biogasification Facilities of Food Waste*; Ministry of Environment: Sejong, Republic of Korea, 2017.
29. Angelidaki, I.; Alves, M.; Bolzonella, D.; Borzacconi, L.; Campos, J.L.; Guwy, A.J.; Kalyuzhnyi, S.; Jenicek, P.; van Lier, J.B. Defining the biomethane potential (BMP) of solid organic wastes and energy crops: A proposed protocol for batch assays. *Water Sci. Technol.* **2009**, *59*, 927–934. [\[CrossRef\]](#)
30. Oh, S.-Y.; Yoon, Y.-M. Energy recovery efficiency of poultry slaughterhouse sludge cake by hydrothermal carbonization. *Energies* **2017**, *10*, 1876. [\[CrossRef\]](#)
31. Lay, J.-J.; Li, Y.-Y.; Noike, T. Mathematical model for methane production from landfill bioreactor. *J. Environ. Eng.* **1998**, *124*, 730–736. [\[CrossRef\]](#)
32. Luna-de-Risco, M.; Normak, A.; Orupöld, K. Biochemical methane potential of different organic wastes and energy crops from Estonia. *Agron. Res.* **2011**, *9*, 331–342.
33. Sørensen, A.H.; Winther-Nielsen, M.; Ahring, B.K. Kinetics of lactate, acetate and propionate in unadapted and lactate-adapted thermophilic, anaerobic sewage sludge: The influence of sludge adaptation for start-up of thermophilic UASB-reactors. *Appl. Microbiol. Biotechnol.* **1991**, *34*, 823–827. [\[CrossRef\]](#)
34. Rice, E.; Baird, R.; Eaton, A.; Clesceri, L. *APHA (American Public Health Association): Standard Method for the Examination of Water and Wastewater*; AWWA (American Water Works Association) and WEF (Water Environment Federation): Washington, DC, USA, 2012.
35. Duncan, D.B. Multiple range and multiple F tests. *Biometrics* **1955**, *11*, 1–42. [\[CrossRef\]](#)
36. Yuan, T.; Bian, S.; Ko, J.H.; Liu, J.; Shi, X.; Xu, Q. Exploring the roles of zero-valent iron in two-stage food waste anaerobic digestion. *Waste Manag.* **2020**, *107*, 91–100. [\[CrossRef\]](#) [\[PubMed\]](#)
37. Meng, X.; Zhang, Y.; Li, Q.; Quan, X. Adding Fe⁰ powder to enhance the anaerobic conversion of propionate to acetate. *Biochem. Eng. J.* **2013**, *73*, 80–85. [\[CrossRef\]](#)
38. Wang, Y.; Wang, D.; Fang, H. Comparison of enhancement of anaerobic digestion of waste activated sludge through adding nano-zero valent iron and zero valent iron. *RSC Adv.* **2018**, *8*, 27181–27190. [\[CrossRef\]](#)
39. Zhang, J.; Wang, Z.; Lu, T.; Liu, J.; Wang, Y.; Shen, P.; Wei, Y. Response and mechanisms of the performance and fate of antibiotic resistance genes to nano-magnetite during anaerobic digestion of swine manure. *J. Hazard. Mater.* **2019**, *366*, 192–201. [\[CrossRef\]](#) [\[PubMed\]](#)
40. Ye, W.; Lu, J.; Ye, J.; Zhou, Y. The effects and mechanisms of zero-valent iron on anaerobic digestion of solid waste: A mini-review. *J. Clean. Prod.* **2021**, *278*, 123567. [\[CrossRef\]](#)
41. Yang, Y.; Guo, J.; Hu, Z. Impact of nano zero valent iron (NZVI) on methanogenic activity and population dynamics in anaerobic digestion. *Water Res.* **2013**, *47*, 6790–6800. [\[CrossRef\]](#)
42. Kong, X.; Wei, Y.; Xu, S.; Liu, J.; Li, H.; Liu, Y.; Yu, S. Inhibiting excessive acidification using zero-valent iron in anaerobic digestion of food waste at high organic load rates. *Bioresour. Technol.* **2016**, *211*, 65–71. [\[CrossRef\]](#)

43. Zhang, Y.; Yang, Z.; Xu, R.; Xiang, Y.; Jia, M.; Hu, J.; Zheng, Y.; Xiong, W.; Cao, J. Enhanced mesophilic anaerobic digestion of waste sludge with the iron nanoparticles addition and kinetic analysis. *Sci. Total Environ.* **2019**, *683*, 124–133. [[CrossRef](#)]
44. Jing, Y.; Wan, J.; Angelidaki, I.; Zhang, S.; Luo, G. iTRAQ quantitative proteomic analysis reveals the pathways for methanation of propionate facilitated by magnetite. *Water Res.* **2017**, *108*, 212–221. [[CrossRef](#)]
45. Yin, Q.; Miao, J.; Li, B.; Wu, G. Enhancing electron transfer by ferroferric oxide during the anaerobic treatment of synthetic wastewater with mixed organic carbon. *Int. Biodeterior. Biodegrad.* **2017**, *119*, 104–110. [[CrossRef](#)]
46. Akturk, A.S.; Demirel, G.N. Improved food waste stabilization and valorization by anaerobic digestion through supplementation of conductive materials and trace elements. *Sustainability* **2020**, *12*, 5222. [[CrossRef](#)]
47. Straub, K.L.; Benz, M.; Schink, B. Iron metabolism in anoxic environments at near neutral pH. *FEMS Microbiol. Ecol.* **2001**, *34*, 181–186. [[CrossRef](#)] [[PubMed](#)]
48. Xu, R.-z.; Fang, S.; Zhang, L.; Huang, W.; Shao, Q.; Fang, F.; Feng, Q.; Cao, J.; Luo, J. Distribution patterns of functional microbial community in anaerobic digesters under different operational circumstances: A review. *Bioresour. Technol.* **2021**, *341*, 125823. [[CrossRef](#)] [[PubMed](#)]
49. Daniels, L.; Belay, N.; Rajagopal, B.S.; Weimer, P.J. Bacterial methanogenesis and growth from CO₂ with elemental iron as the sole source of electrons. *Science* **1987**, *237*, 509–511. [[CrossRef](#)]
50. Dinh, H.T.; Kuever, J.; Mußmann, M.; Hassel, A.W.; Stratmann, M.; Widdel, F. Iron corrosion by novel anaerobic microorganisms. *Nature* **2004**, *427*, 829–832. [[CrossRef](#)]
51. Xu, W.; Zhao, H.; Cao, H.; Zhang, Y.; Sheng, Y.; Li, T.; Zhou, S.; Li, H. New insights of enhanced anaerobic degradation of refractory pollutants in coking wastewater: Role of zero-valent iron in metagenomic functions. *Bioresour. Technol.* **2020**, *300*, 122667. [[CrossRef](#)]
52. Zheng, S.; Yang, F.; Huang, W.; Lei, Z.; Zhang, Z.; Huang, W. Combined effect of zero valent iron and magnetite on semi-dry anaerobic digestion of swine manure. *Bioresour. Technol.* **2022**, *346*, 126438. [[CrossRef](#)]
53. Zhao, Z.; Li, Y.; Yu, Q.; Zhang, Y. Ferroferric oxide triggered possible direct interspecies electron transfer between *Syntrophomonas* and *Methanosaeta* to enhance waste activated sludge anaerobic digestion. *Bioresour. Technol.* **2018**, *250*, 79–85. [[CrossRef](#)] [[PubMed](#)]
54. Lim, E.Y.; Tian, H.; Chen, Y.; Ni, K.; Zhang, J.; Tong, Y.W. Methanogenic pathway and microbial succession during start-up and stabilization of thermophilic food waste anaerobic digestion with biochar. *Bioresour. Technol.* **2020**, *314*, 123751. [[CrossRef](#)]
55. Jang, H.M.; Kim, J.H.; Ha, J.H.; Park, J.M. Bacterial and methanogenic archaeal communities during the single-stage anaerobic digestion of high-strength food wastewater. *Bioresour. Technol.* **2014**, *165*, 174–182. [[CrossRef](#)] [[PubMed](#)]
56. Lee, J.; Kim, E.; Han, G.; Tongco, J.V.; Shin, S.G.; Hwang, S. Microbial communities underpinning mesophilic anaerobic digesters treating food wastewater or sewage sludge: A full-scale study. *Bioresour. Technol.* **2018**, *259*, 388–397. [[CrossRef](#)] [[PubMed](#)]

Disclaimer/Publisher's Note: The statements, opinions and data contained in all publications are solely those of the individual author(s) and contributor(s) and not of MDPI and/or the editor(s). MDPI and/or the editor(s) disclaim responsibility for any injury to people or property resulting from any ideas, methods, instructions or products referred to in the content.